This copy is for personal use only. To order printed copies, contact *reprints@rsna.org*

Radiology

Progressive Reduction in Gray Matter in Patients with Schizophrenia Assessed with MR Imaging by Using Causal Network Analysis[1]

Yuchao Jiang, PhD
Cheng Luo, PhD
Xin Li, MS
Mingjun Duan, MD
Hui He, PhD
Xi Chen, PhD
Hang Yang, PhD
Jinnan Gong, PhD
Xin Chang, MS
Marie Woelfer, MD
Bharat B. Biswal, PhD
Dezhong Yao, PhD

An earlier incorrect version of this article appeared online. This article was corrected on March 5, 2018.

[1] From the Clinical Hospital of Chengdu Brain Science Institute, Ministry of Education Key Laboratory for Neuroinformation, University of Electronic Science and Technology of China, Second North Jianshe Road, Chengdu 610054, China (Y.J., C.L., X.L., M.D., H.H., X. Chen, H.Y., J.G., X. Chang, B.B.B., D.Y.); High-Field Magnetic Resonance Brain Imaging Key Laboratory of Sichuan Province, School of Life Science and Technology, Center for Information in Medicine, University of Electronic Science and Technology of China, Chengdu, China (Y.J., C.L., M.D., H.H., X. Chen, H.Y., J.G., D.Y.); and Department of Biomedical Engineering, New Jersey Institute of Technology, Newark, NJ (M.W., B.B.B.).
Received August 17, 2017; revision requested October 18; revision received November 7; accepted November 9; final version accepted November 9. **Address correspondence to** C.L. (e-mail: *chengluo@uestc.edu.cn*).

Study supported by the National Natural Science Foundation of China (81330032, 81471638, 81771822) the Chinese Fundamental Research Funding for Central Universities in the University of Electronic Science and Technology of China (ZYGX2016J124), the Sixth Science and Technology Project (2013) from the Chengdu Science and Technology Bureau (2013-11), and the Sichuan Province Science and Technology Support Project (2017SZ0004).

© RSNA, 2018

Purpose: To investigate the temporal and causal relationships of structural changes in the brain in patients with schizophrenia.

Materials and Methods: T1-weighted magnetic resonance (MR) images of 97 patients with schizophrenia (29 women; mean ± standard deviation age, 41 years ± 11.5; range, 16–66 years; illness duration, 16.3 years ± 10.9; range, 0–50 years) and 126 age- and sex-matched (38 years ± 14.9; range, 18–68 years; 42 women) healthy control subjects were evaluated. The causal network of structural covariance was used to assess the causal relationships of structural changes in patients with schizophrenia. This was accomplished by applying Granger causality analysis to the morphometric T1-weighted images ranked according to duration of disease.

Results: With greater disease duration, reduction in gray matter volume began in the thalamus and progressed to the frontal lobe, and then to the temporal and occipital cortices as well and the cerebellum ($P < .00001$, false discovery rate corrected). The thalamus was shown to be the primary hub of the directional network and exhibited positive causal effects on the frontal, temporal, and occipital regions as well as on the cerebellum ($P < .05$, false discovery rate corrected). The frontal regions, which were identified to be transitional points, projected causal effects to the occipital lobe, temporal regions, and the cerebellum and received causal effects from the thalamus ($P < .05$, false discovery rate corrected).

Conclusion: Schizophrenia shows progression of gray matter abnormalities over time, with the thalamus as the primary hub and the frontal regions as prominent nodes.

© RSNA, 2018

Online supplemental material is available for this article.

Schizophrenia (SZ) is a common psychiatric disorder characterized by a multidimensional psychotic syndrome (1). Morphometric studies have revealed gray matter (GM) volume atrophy in subcortical regions of the thalamus and basal ganglia and cortical GM including the frontal, temporal, and occipital lobes as well as the cerebellum (2,3), indicating the importance of multiregional abnormalities in the pathologic mechanism of SZ. It is currently hypothesized that as a developmental disorder, SZ shows progressive impairments in cerebral morphology and connectivity (4). Therefore, investigating the interregional relationship of progressive brain damage is necessary to understand the pathologic deviations of neurodevelopment in patients with SZ.

Structural covariance network (SCN) techniques have been introduced to quantitatively determine whether a morphometric change in one region correlates with changes in other regions (5,6). SCN has been applied to investigate the network characteristics and the structural covariance connectivity in multiple diseases including SZ (7). Studies have demonstrated abnormal segregation among the prefrontal cortex and somatosensory and occipital regions with use of the SCN (8). Authors of these studies have effectively mapped the topologic patterns of concomitant changes among brain regions and coordinated developmental processes of brain abnormalities in patients with SZ. However, one limitation of the SCN method is that it involves correlation analysis (zero time-lagged correlation) to measure the synchronization; therefore, it cannot allow quantification of the possible causal relationships between different brain regions (ie, whether the damage in one region precedes that in another).

Implication for Patient Care

- The thalamus is implicated as the primary hub of progressive gray matter abnormalities that subsequently progress to other regions of the brain.

Granger causality (GC) analysis is another common technique that can allow delineation of information flow through detection of whether neural activity in one region precedes and allows prediction of the activity in another region. GC analysis is widely used in functional time-series data analysis for several neuropsychiatric disorders such as SZ (9,10), social anxiety disorder (11), and epilepsy (12). When morphometric data are ranked according to progression, information such as disease duration, and given temporal information, GC analysis can be applied to these sequenced data to assess the causal relationships of structural alterations among brain regions. This approach, named causal structural covariance network (CaSCN) analysis, was used in a recent epilepsy study (13). Therefore, we hypothesized that the CaSCN could be used to characterize the progressive alterations of the structural brain network in patients with SZ. In our study, we aimed to investigate the progressive profiles of the structural network throughout the duration of the illness and to further evaluate the causal effect of structural changes in patients with SZ by using the CaSCN.

Materials and Methods

Participants

The study was approved by the Ethics Committee of the Clinical Hospital of Chengdu Brain Science Institute (Chengdu Mental Health Center), and all subjects provided written informed consent after they were given a complete description of the study. Ninety-seven patients with SZ (68 men; mean ± standard deviation age, 41.0 years ± 11.5; range, 16–66 years; mean illness duration, 16.3 years ± 10.9; range, 0–50 years) were recruited from the Clinical Hospital of Chengdu Brain Science Institute. Each patient was diagnosed on the basis of the Diagnostic and Statistical Manual of Mental Disorders, Fourth Edition (DSM-IV). Subjects with a history of brain injuries, substance-related disorders, and major medical or neurologic disorders were excluded. To exclude the potential effect of similar genetic backgrounds, history of a psychiatric disorder in a first- or second-degree relative was an additional exclusion criterion for healthy control subjects. All patients were taking medication (eg, antipsychotics and neuroleptics: olanzapine [n = 4], clozapine [n = 52], quetiapine [n = 12], risperidone [n = 29], haloperidol [n = 6], ziprasidone [n = 6], aripiprazole [n = 13]). To evaluate the effects of various antipsychotic drugs, we used a standardized quantitative formula for each antipsychotic medication to determine equivalents to chlorpromazine (14). The chlorpromazine equivalent dose of the antipsychotics was 324.5 mg per day ± 157.1. A sample of 126 healthy control subjects (84 men and 42 women; age, 38 years ± 14.9), matched to the patient group according to age and sex was also recruited in this study. The healthy control subjects were also matched with the patients with SZ in handedness (one left-handed and 125 right-handed healthy control subjects, three left-handed and 94 right-handed patients with SZ; P = .20, χ^2 test) and

https://doi.org/10.1148/radiol.2017171832

Content codes: MR NR

Radiology 2018; 0:1–10

Abbreviations:
CaSCN = causal SCN
GC = Granger causality
GM = gray matter
ROI = region of interest
SCN = structural covariance network
SZ = schizophrenia

Author contributions:
Guarantors of integrity of entire study, Y.J., C.L., M.D., H.H., X. Chen, J.G., D.Y.; study concepts/study design or data acquisition or data analysis/interpretation, all authors; manuscript drafting or manuscript revision for important intellectual content, all authors; approval of final version of submitted manuscript, all authors; agrees to ensure any questions related to the work are appropriately resolved, all authors; literature research, C.L., X.L., M.D., H.Y., J.G., X. Chang, M.W., B.B.B., D.Y.; clinical studies, C.L., M.D., X. Chen, B.B.B., D.Y.; experimental studies, C.L., M.D., D.Y.; statistical analysis, Y.J., C.L., X.L., H.H., H.Y., X. Chang, B.B.B., D.Y.; and manuscript editing, Y.J., C.L., X.L., M.D., H.H., X. Chang, M.W., B.B.B., D.Y.

Conflicts of interest are listed at the end of this article.

years of education (SZ, 11.8 years ± 3.1; healthy control subjects, 10.9 years ± 3.4; $P = .08$, two sample t test). The magnetic resonance (MR) imaging anatomic images were evaluated by two experienced radiologists (C.L. and W.Y., each with more than 10 years of experience in radiology) to exclude subjects with gross brain abnormalities. Four patients with SZ and one healthy control subject were excluded because they were unable to complete MR imaging. Some of the patients were part of previous studies (9,15–17). Twenty-eight of the 97 patients were included in a prior study in which the authors identified abnormal functional integration in the basal ganglia network by using spatial independent component analysis (15). The same 28 patients were also included in a prior article in which the authors found functional disconnection between the visual cortex and the sensorimotor cortex by using functional connectivity density analysis (16). Forty-six of the 97 patients were previously included in a prior article in which authors demonstrated dysfunction in the insula with data-driven clustering and functional connectivity analysis (17). Sixty-nine of the 97 patients were included in a prior article in which the authors identified an altered hippocampus-cerebellum-cortical circuit with a combination of local consistency analysis and GC analysis (9). All of these previous studies were investigations of brain dysfunctions in which resting-state functional MR imaging data were used, whereas our study was focused on progressive brain morphologic abnormalities in which structural MR imaging data were used (T1-weighted images).

Image Acquisition

A 3-T MR imager (Discovery MR 750; GE Healthcare, Milwaukee, Wis) was used to collect imaging data in the University of Electronic Science and Technology of China. High-spatial-resolution T1-weighted images were acquired by using a three-dimensional fast spoiled gradient-echo sequence. The main parameters included repetition time msec/echo time msec, 6.008/1.984; flip angle, 90°; field of view, 25.6 × 25.6 cm; matrix size, 256 × 256; section thickness, 1 mm (no gap). A functional MR imaging sequence was also performed but not used in our study.

Data Preprocessing

High-spatial-resolution T1-weighted MR imaging data were processed with standard voxel-based morphometry by using the Computational Anatomy Toolbox (CAT12; *http://dbm.neuro.uni-jena.de/cat12/*) in statistical parametric mapping software (SPM12; *http://www.fil.ion.ucl.ac.uk/spm/*). First, all images were checked for artifacts and reoriented to adjust image origins at the anterior commissure. Second, T1-weighted images were normalized to Montreal Neurologic Institute space; segmented into GM, white matter, and cerebrospinal areas; and resampled to a volume image resolution of 2 × 2 × 2 mm^3. After the data quality and sample homogeneity were checked, the segmented GM images were smoothed by using an 8-mm full width at half maximum Gaussian kernel. Finally, the GM optimal threshold mask, created with data from all subjects, was applied to eliminate non-GM voxels (18). The generated smoothed GM images were used as the GM volume for subsequent group comparisons.

Voxel-based Morphometric Analysis: Overall and Stage-specific Atrophy Patterns in SZ

To estimate the overall GM volume alterations in patients with SZ, the two sample t test implemented in SPM12 was performed between the GM images of SZ and healthy control subject groups ($P < .00001$, false discovery rate corrected). Subsequently, to map the progressive patterns of GM volume atrophy in the SZ, we used stage-specific procedures that have been used in previous works (13). All patients were categorized into three subgroups according to the progressive stage of SZ duration (stage 1, 0–10 years; stage 2, 11–20 years; and stage 3, > 20 years). Then, GM volume images of each subgroup were compared with those of healthy control subjects by using a two-sample t test ($P < .00001$, false discovery rate corrected). Ten two-sample t tests were performed; thus we applied a strict threshold P value of less than .00001 after false discovery rate correction for each t map to account for the increase in the probability of false-positive results; the threshold corresponds to a P value of less than .0001 after Bonferroni correction. To ensure that any differences were not due to an arbitrary strategy, we also categorized all patients into six subgroups according to duration of disease (0–5 years, 5–10 years, 10–15 years, 5–20 years, 20–25 years, and > 25 years) to further verify the results. Sex and age were regressed as covariates in these analyses. In addition, to investigate the relationship between atrophy magnitude and SZ duration, voxel-wise Spearman correlation analysis was performed ($P < .05$, false discovery rate corrected).

Mapping Causal Effect of GM Atrophy Pattern in SZ by Using Seed-based CaSCN

The analysis pipeline for the CaSCN was similar to that used in the original study by Zhang and colleagues (13) and is only briefly described here. The GM volume data of all patients were sequenced according to the ranks of the SZ duration from low to high. This data sequencing was analogous to time-series information for characterizing the progressive property of SZ on the basis of cross-sectional data. Subsequently, similar to GC analysis applied in functional MR imaging data analysis, the pseudo–time series was used to construct seed-based CaSCN. The seed region was selected from the previously mentioned voxel-based morphometric analysis. Signed-path coefficient GC analysis implemented with an MR imaging toolkit (REST; *http://www.restfmri.net*) was performed on a voxel-wise basis for all the voxels in the mask of the brain areas with reduced GM volume. The signed-path coefficient GC analysis has been used previously to investigate directed influences between two regions and has been used in patients with SZ undergoing functional MR imaging (9,19). Similarly, the CaSCN could allow assessment of the causal effect of GM volume alteration

Figure 1

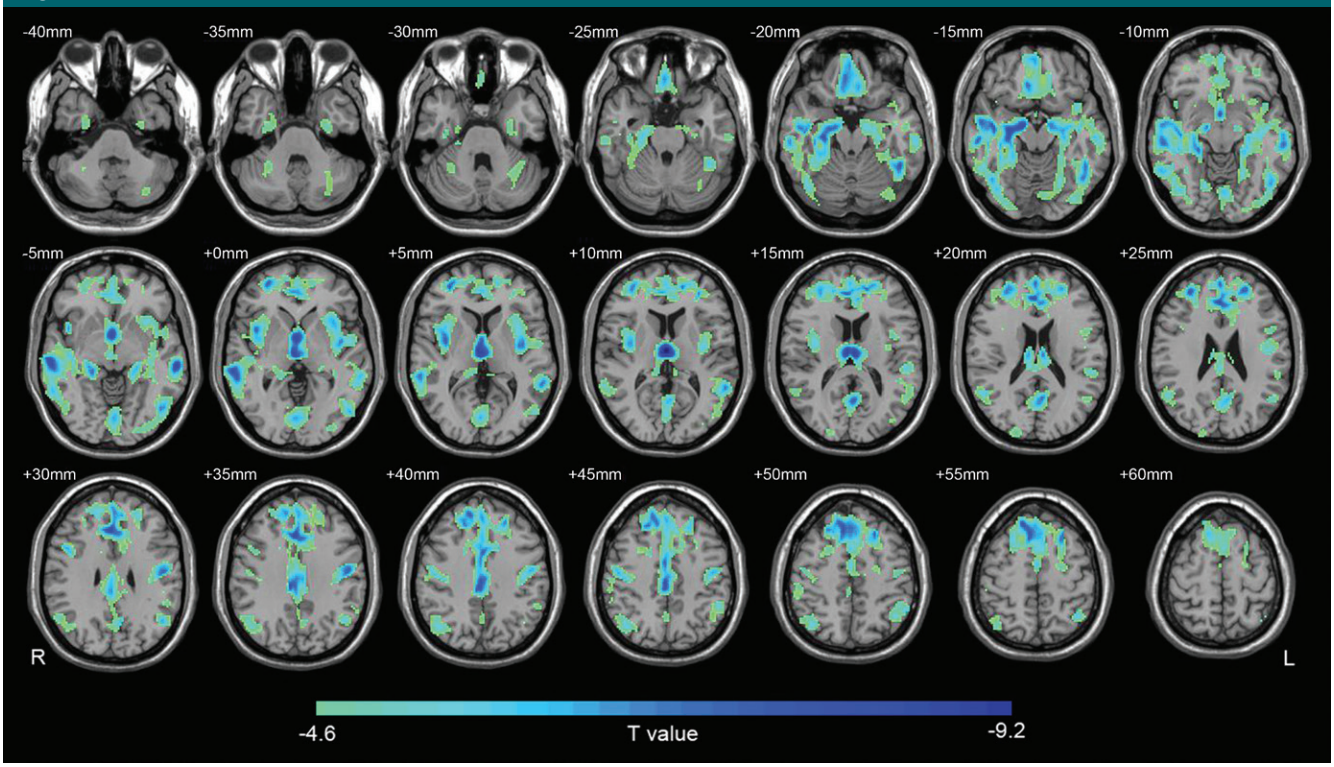

Figure 1: MR images show reduced gray matter volume in patients with schizophrenia. Reduced gray matter volume (blue) images are overlaid on an axial template, with coordinate planes in white. Color bar represents *t* values from two-sample *t* test.

of a region on the other regions. As the seed exhibited the reduction of GM volume in SZ, a positive Granger causality (GC) value indicated that the same GM volume alteration (reduced) in the regions lagged behind the seed atrophy, which may suggest the reduction is driven by the seed. A negative GC value denoted that regions with an opposite alteration (increased) lagged behind the seed atrophy, which may imply a compensatory effect. Sex, age, total intracranial volume, and time interval between two pseudo–time points were regressed as covariates in conducting CaSCN analysis. To present statistical significance, the GC map was transformed to a *z* score map and the threshold was presented at a *z* score of greater than 2.3 and a GC value of greater than 0.16. This corresponded to a *P* value of .05, false discovery rate corrected (13).

To further investigate the causal effect among the regions of interest (ROI) obtained from CaSCN analysis, we also calculated an ROI-to-ROI GC analysis, as originally proposed by Zhang and colleagues (13). The signed-path coefficient GC analysis was performed to construct an ROI-wise causal network that characterized causal relationships among ROIs. To maintain consistency with the voxel-wise CaSCN analysis, the same threshold was set at a GC value of greater than 0.16. The binary (weighted) "out-degree" and "in-degree" values (in-degree value = the number of head ends adjacent to a node, out-degree value = number of tail ends adjacent to a node) of each ROI were computed separately. The binary (weighted) in-degree value of an ROI represents the sum of the number (strength) of paths projecting to the ROI. The binary (weighted) out-degree value of a node refers to the sum of the number (strength) of paths projecting to other nodes. In addition, the out-in degree was also calculated as the subtraction between out-degree and in-degree values to identify the causal targets or causal source levels.

Results

GM Atrophy Pattern

Compared with the healthy control subjects, the patients with SZ showed reduced GM volume in the thalamus, basal ganglia, frontal lobe, insula, pre- and postcentral gyrus, bilateral temporal gyrus, occipital cortex, and cerebellum (Fig 1). No region with increased GM volume was observed in the SZ group. Detailed regions are provided in Table E1 (online). Correlation analysis between reduced GM volume and SZ duration demonstrated that longer disease duration was related to lower GM volume. These areas included the bilateral frontal lobe, middle cingulate gyrus, left inferior parietal lobule, left postcentral gyrus, right

Figure 2

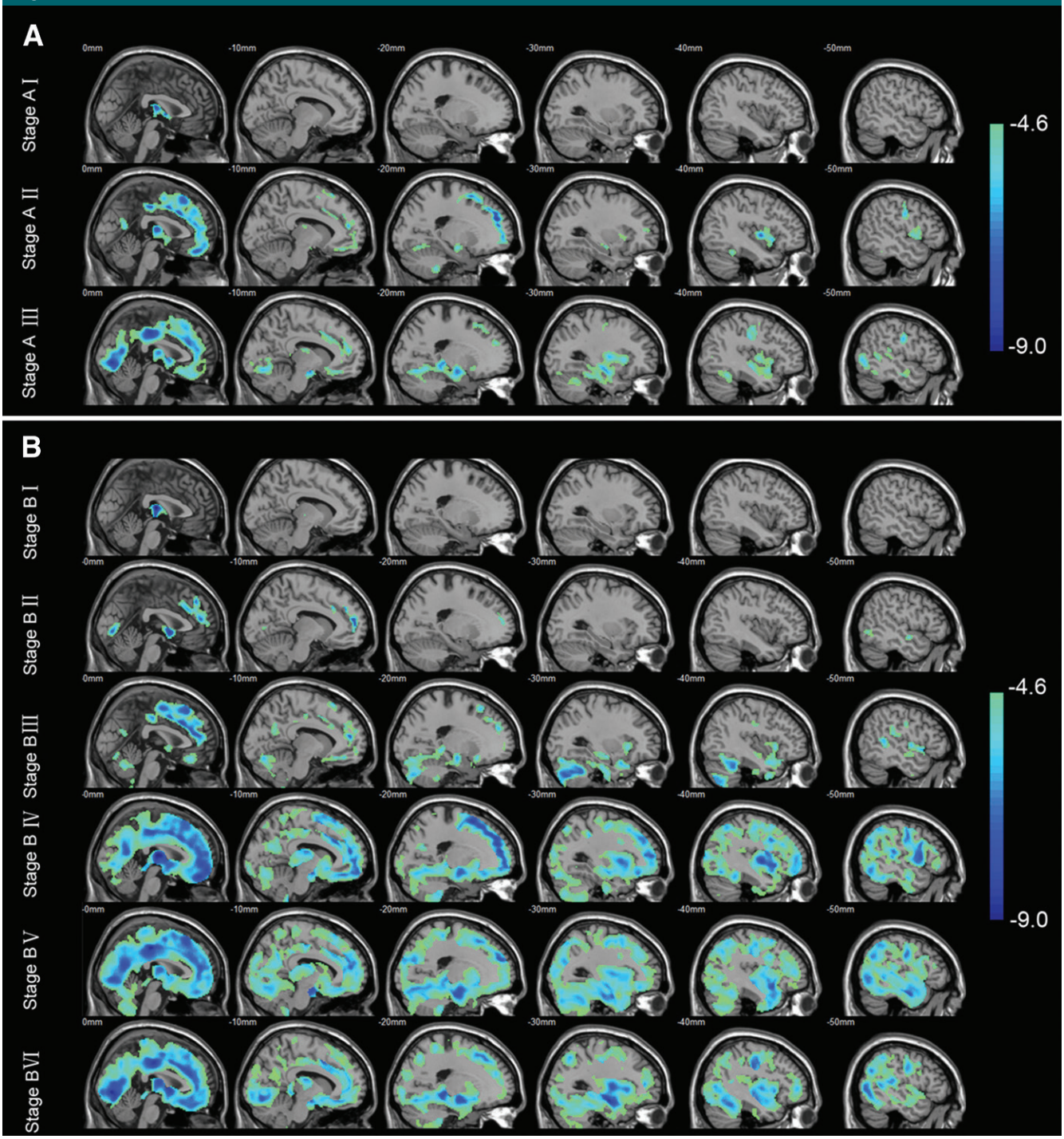

Figure 2: MR images show stage-specific gray matter volume reductions in patients with schizophrenia (SZ) relative to the healthy controls. Reduced gray matter volume images were overlaid on a sagittal template, with coordinate planes in white. Color bar represents *t* values from two-sample *t* test. *A*, Subjects with SZ were categorized into three subgroups according to SZ duration (*stage AI*, 0–10 years; stage *AII*, 11–20 years; stage *AIII*, > 20 years). *B*, All patients were categorized into six subgroups (stage *BI*, 0–5 years; *BII*, 5–10 years; *BIII*, 10–15 years; *BIV*, 15–20 years; *BV*, 20–25 years; *BVI*, > 25 years).

lingual gyrus, and bilateral putamen as well as the cerebellum (Table E2 and Fig E1 [online]).

Stage-specific Atrophy Patterns in Patients with SZ

To map the progressive patterns of GM volume atrophy in patients with SZ, stage-specific procedures were used by grouping patients into several subgroups according to SZ duration. Progressive atrophy patterns were observed in areas of the thalamus; frontal, temporal, and occipital cortical regions; and the cerebellum. At stage 1 (n = 36, 20 men; mean age, 32.9 years ± 10.9; age range, 16–66 years), only the thalamus exhibited reduced GM volume. At stage 2 (n = 27, 16 men; mean age, 42.8 years ± 7.1; age range, 27–55 years), in addition to the thalamus, the following regions showed a GM volume decrease: the orbital frontal cortex, medial and lateral prefrontal lobe, cingulate cortex, insula, pre- and postcentral gyrus, and premotor cortex. Finally, at stage 3 (n = 30, 29 men; mean age, 49.0 years ± 8.3; age range, 27–65 years), in addition to the above areas, the occipital cortex, temporal cortex, and cerebellum exhibited GM volume decrease. In general, with longer SZ duration, regions with GM volume reductions expanded from the thalamus (stage 1) to the frontal lobe (stage 2), and then to the temporal lobe, occipital cortex, and the cerebellum (stage 3) (Fig 2). Detailed results are provided in Table E3 and Figure E2 (online).

We further evaluated the relationship between GM volume reductions in each stage and disease duration. We found that atrophy in the medial prefrontal cortex and left orbitofrontal cortex was negatively correlated with disease duration at stage 1. The GM volume reduction in the postcentral gyrus was negatively associated with disease duration at stage 2 (Table E4 and Fig E3 [online]). At stage 3, disease duration was not correlated with GM volume alterations in any region (all P values > .05). With the use of another categorized strategy in which patients were divided into six subgroups according to disease (0–5 years, 5–10 years, 10–15 years, 15–20 years, 20–25 years, and > 25 years) similar alteration patterns were exhibited (compare Fig 2, *B*).

Figure 3

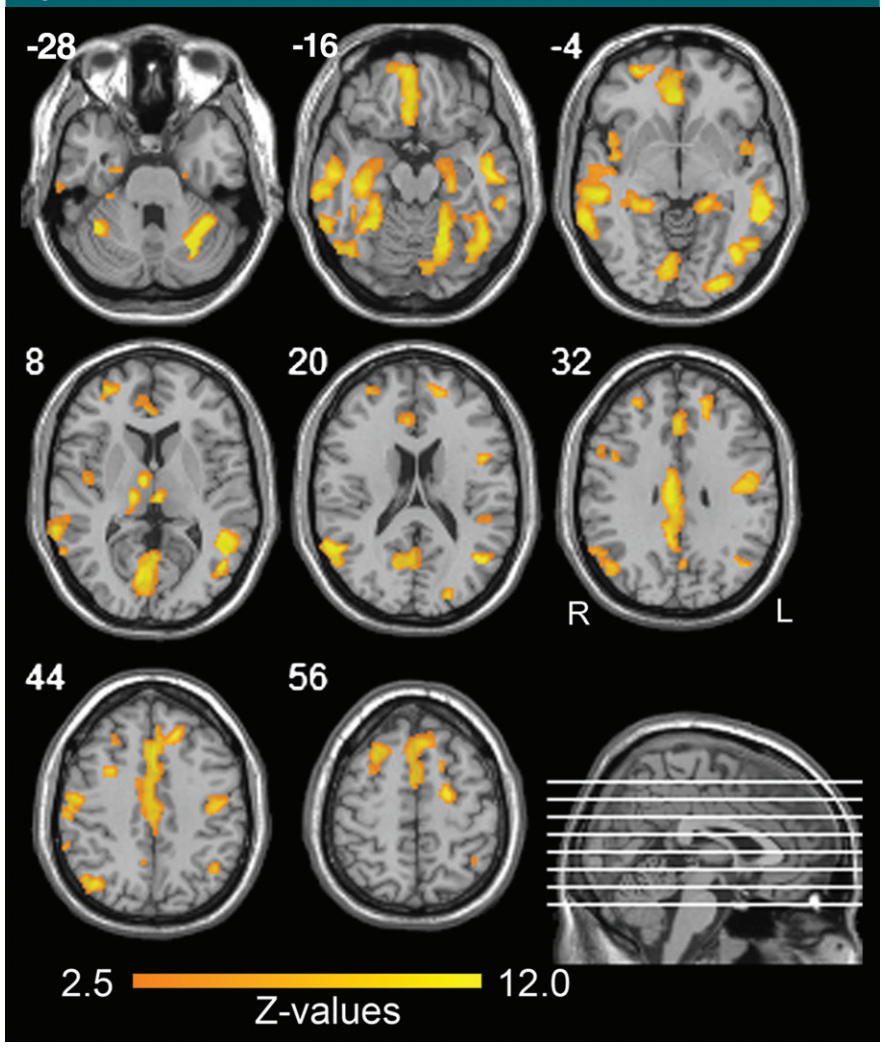

Figure 3: Causal networks show causal effects of gray matter atrophy pattern in patients with schizophrenia (SZ). Causal networks were constructed by applying Granger causality (GC) analysis to sequenced morphometric data according to the ranks of SZ duration from low to high. The thalamus (Montreal Neurologic Institute coordinates: 1, −13, 10) was used as the seed region on the basis of voxel-based morphometric analysis. Considering the reduction in the gray matter volume of thalamus in patients with SZ, regions with positive GC values indicate the same gray matter volume alteration (reduction) lagged behind thalamus atrophy, which may suggest that it is driven by the thalamus. GC values were transformed to z values.

Mapping Causal Effects of GM Atrophy Pattern in Patients with SZ

To characterize the causal effect of progressive GM volume atrophy in patients with SZ, the CaSCN was constructed with the thalamus as the seed, since it was reduced in the first stage. The thalamus region (Montreal Neurologic Institute coordinates: 1, −13, 10) was selected from a two-sample t test of a whole-brain voxel-based morphometric comparison among all patients and healthy control subjects. CaSCN results demonstrated positive GC from the seed in the thalamus to the frontal lobe, cingulate cortex, insula, pre- and postcentral gyrus, temporal-parietal junction,

Regions Showing Causal Effect from the Seed of Thalamus by Using CaSCN Analysis

Region	Montreal Neurologic Institute Coordinates	Grainger Causality Value	*z* Value	Cluster (Voxels)
Fusiform, left	−24, −56, −16	0.47	6.73	2887a
Fusiform, right	32, −44, −21	0.41	5.71	1271b
Cerebellum 6, right	31, −48, −29	0.44	6.16	2887a
Cerebellum 6, left	−35, −52, −29	0.43	6.09	2887a
Temporoparietal junction, right	51, −54, 25	0.42	5.94	439c
Temporoparietal junction, left	−49, −61, 18	0.35	4.87	2887a
Inferior temporal gyrus, left	−49, −49, −19	0.41	5.78	2887a
Inferior temporal gyrus, right	55, −49, −5	0.28	3.85	2887a
Dorsal medial prefrontal cortex	26, 11, 49	0.39	5.41	212
Middle temporal gyrus, left	−62, −37, −5	0.38	5.38	2887a
Middle temporal gyrus, right	51, −13, −13	0.31	4.28	1522b
Lingual gyrus	6, −74, 3	0.37	5.18	2927d
Middle cingulate cortex	2, −12, 37	0.36	5.05	2927d
Dorsal medial prefrontal cortex	−5, 21, 43	0.35	4.92	2927d
Angular gyrus, right	40, −72, 37	0.33	4.73	439c
Hippocampus, right	34, −30, −10	0.33	4.53	1271e
Hippocampus, left	−27, −36, −8	0.32	4.45	2887a
Insula, right	40, −10, 1	0.30	4.19	1522
Superior frontal gyrus, right	25, 56, 5	0.29	3.94	1143f
Ventral medial prefrontal cortex	−1, 41, −13	0.28	3.81	1143f
Posterior cingulate cortex	4, −48, 31	0.28	3.84	2927d
Postcentral gyrus, left	−51, −12, 39	0.26	3.60	354
Orbital frontal cortex	0, 56, −14	0.24	3.29	1143f

Note.—Numbers followed by the same lowercase letter (a-f) mean that these regions shared the same clusters. *CaSCN* = causal structural covariance network.

angular and temporal gyrus, hippocampus, fusiform, and cerebellum (Fig 3 and Table 1). This indicates that the thalamus may be the hub of the directional network in terms of out-degree values, and may exhibit positive causal effects to other regions, thus potentially exerting a damaging effect to other regions. These regions were extracted to use for the ROI-to-ROI CaSCN analysis. No negative GC was observed from the seed to other regions. Also, no causal effects from other regions to the seed in the thalamus were found.

The ROI-to-ROI results exhibited a directional network that revealed an interregional causal relationship (Fig 4). The frontal nodes including the dorsolateral prefrontal cortex, orbitofrontal cortex, ventromedial prefrontal cortex, and middle cingulate cortex mainly projected causal effects to the occipital lobe, temporal regions, and the cerebellum (ie, out-degree hubs) and received causal effects from the thalamus, which were identified to be transition points. The nodes in the temporal lobe, occipital cortex, and the cerebellum received more causal effect from other nodes (ie, in-degree hubs), which were identified as the causal targets.

Discussion

By using T1-weighted structural data, we evaluated the causal relationship between brain regions with progressive morphometric alterations in patients with SZ by using the CaSCN. Duration of illness was associated with GM volume reductions progressing from the thalamus to the frontal lobe, and then to temporal, occipital, and cerebellar regions. A directional network demonstrated that the thalamus was its hub; changes in the thalamus were potentially causally related to all other nodes. The frontal nodes, which were identified to be transition points, received causal effects from the thalamus and projected causal effects to other regions. The temporal, occipital, and cerebellar regions received more causal effects from other nodes and were identified as the causal targets. The pattern of the CaSCN was generally in line with results of the stage-specific comparative analysis.

Changes in brain structure over time are best evaluated in longitudinal studies (20). However, results from this work suggest the potential for assessing temporal changes in the structure of the brain by applying GC analysis to morphometric data classified according to illness duration. In spite of antipsychotic medication or epiphenomena related to the disease (21), illness duration can be used as a surrogate parameter for describing the progression of SZ. A pseudo–time series and lifespan information of illness progression may be generated by incorporating information on disease duration. The CaSCN revealed that structural changes in one region precede and allow prediction of the change in another region in relationship to the duration of illness (ie, a potential causal effect). Consistent

Figure 4

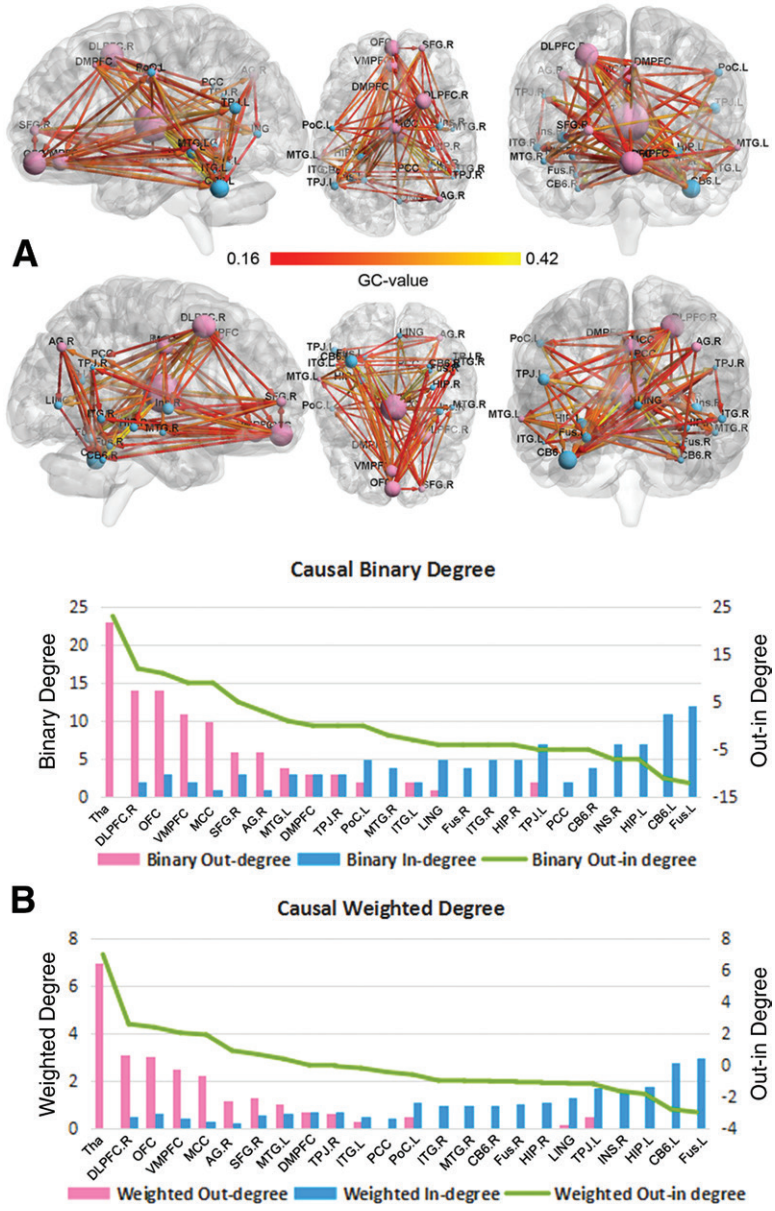

Figure 4: Region-of-interest (ROI)–based causal structural covariance network analysis shows causal relationship among ROIs. *A*, Bivariate signed-path coefficient Granger causality analysis was performed to construct an ROI-wise causal network to characterize causal relationships among ROIs. *B*, The binary (weighted) out- and in-degree value of each ROI was computed separately. In detail, the binary (weighted) in-degree value of a ROI represents the sum of the number (strength) of paths that project to itself. The binary (weighted) out-degree value of a node refers to the sum of the number (strength) of paths that project to other nodes. In addition, the out-in degree value was also calculated as the subtraction between out-degree and in-degree values to identify the causal targets or causal source levels. *AG* = angular gyrus, *CB6* = cerebellum 6, *DLPFC* = dorsal lateral prefrontal cortex, *DMPFC* = dorsal medial prefrontal cortex, *Fus* = fusiform, *HIP* = hippocampus, *INS* = insula, *ITG* = inferior temporal gyrus, *L* = left, *LING* = lingual gyrus, *MCC* = middle cingulate cortex, *MTG* = middle temporal gyrus, *OFC* = orbital frontal cortex, *PCC* = posterior cingulate cortex, *PoC* = postcentral gyrus, *R* = right, *SFG* = superior frontal gyrus; *TPJ* = temporoparietal junction, *VMPFC* = ventral medial prefrontal cortex.

with traditional methods such as stage-specific comparisons (22), The CaSCN captured the reduction in GM from the thalamus to other regions. These results further demonstrated that CaSCN analysis could be an effective method to explore interregional covariance of structural changes in patients with SZ.

Consistent with results of a previous longitudinal study (22), in this study we found progressive GM reductions during particular stages of illness. The illness duration of SZ was associated with GM atrophy progressing from the thalamus to the frontal lobe and then to the temporal lobe, occipital cortices, and the cerebellum. This progressive atrophy pattern in these regions has been observed in patients with a first-episode of or chronic SZ (23–28). In particular stages of illness, lower GM volume in the frontal lobe and the postcentral gyrus was linked to longer disease duration, consistent with results from previous studies (22,29). This progressive atrophy may reach a maximum effect after long duration of illness (> 20 years). In addition, authors of prior studies (30,31) have found that progressive GM loss in patients with SZ was associated with prominent negative symptoms and cognitive impairment. Our findings provide further evidence of progressive GM reductions during different stages of illness duration and further demonstrated an interregional causal relationship.

In our study, the thalamus, as the hub of the directional network, demonstrated positive causal effects on frontal areas, the temporal lobe, occipital regions, and the cerebellum. The thalamus is an essential node that is engaged in the bidirectional flow of neuronal signals between different cortical areas and subcortical regions and has been linked to the processing of cognition and emotion, which are impaired in patients with SZ (32,33). The positive causal value might implicate that regional GM volume reduction of the thalamus precedes that of the other regions. The thalamus connects to different cortical areas as well as the cerebellum (34); GM loss in the thalamus may consecutively lead to neuronal

damage in other regions. Several studies have provided evidence of the crucial role of the frontal cortex in the pathology of SZ and reported that a reduction of GM volume in the prefrontal lobe was associated with cognitive and emotional dysfunction (35). In addition, diffusion-tensor imaging indicated an aberrant frontal-thalamic structural connectivity in patients with SZ (36). In a study (2) in which structural MR imaging and resting-state functional MR imaging were used, authors found that the causal connectivity of the frontal-thalamic circuit might be affected by structural deficits in patients with SZ. Overall, our study results illustrated a potential causal relationship from the thalamus and frontal lobe to further regions with GM atrophy, which might indicate the progressive pathologic process of structural damage in SZ.

Our study had several limitations. First, the underlying physiologic mechanism of disease progression still remains unclear. In addition, temporally organized data do not directly reflect the real temporal sequence of illness progression. Thus, longitudinal studies must be performed to further clarify the causal relationship between structural deficits. Second, although age was regressed as a covariate in CaSCN analysis, its confounding effect on the structural images cannot be excluded. The causal relationships between structural alterations and illness course should be interpreted cautiously. Third, all patients received antipsychotic medication. Therefore, findings may have been confounded by the treatment regimen, antipsychotic therapy, or epiphenomena related to the illness. Fourth, illness duration was used for describing the progression of SZ. Other clinical variables such as severity of illness or response to treatment, which may be related to brain alterations, must be considered in the future (22). Furthermore, stage-specific comparisons were performed by dividing all patients into several subgroups according to stage of illness duration, which was an arbitrary strategy. Finally, the validation of CaSCN analysis results should be verified through replication samples.

The interregional causal effect of structural changes and illness progression in patients with SZ was assessed by using the CaSCN. With greater duration of SZ, GM volume reductions extended from the thalamus to the frontal lobe, and then to the temporal lobe, occipital cortices, and the cerebellum. CaSCN analysis results suggest that the thalamus is the hub of the directional network; the frontal nodes projected causal effect to the occipital lobe, temporal regions, and cerebellum and received the causal effect from the thalamus. These results imply a hierarchy of structural brain damage and an important role of the thalamus and frontal lobe in disease progression. Our work provides further evidence to suggest that SZ is associated with progressive GM abnormalities.

Acknowledgment: We are indebted to Wenjie Yin, MD, Chengdu First People's Hospital, for her help on examination of MR anatomic images.

Disclosures of Conflicts of Interest: Y.J. disclosed no relevant relationships. **C.L.** disclosed no relevant relationships. **X.L.** disclosed no relevant relationships. **M.D.** disclosed no relevant relationships. **H.H.** disclosed no relevant relationships. **X.Chen.** disclosed no relevant relationships. **H.Y.** disclosed no relevant relationships. **J.G.** disclosed no relevant relationships. **X.Chang.** disclosed no relevant relationships. **M.W.** disclosed no relevant relationships. **B.B.B.** disclosed no relevant relationships. **D.Y.** disclosed no relevant relationships.

References

1. Dong D, Wang Y, Chang X, et al. Shared abnormality of white matter integrity in schizophrenia and bipolar disorder: A comparative voxel-based meta-analysis. Schizophr Res 2017;185:41–50.
2. Guo W, Liu F, Liu J, et al. Abnormal causal connectivity by structural deficits in first-episode, drug-naive schizophrenia at rest. Schizophr Bull 2015;41(1):57–65.
3. Haijma SV, Van Haren N, Cahn W, Koolschijn PC, Hulshoff Pol HE, Kahn RS. Brain volumes in schizophrenia: a meta-analysis in over 18 000 subjects. Schizophr Bull 2013;39(5):1129–1138.
4. Rapoport JL, Giedd JN, Gogtay N. Neurodevelopmental model of schizophrenia: update 2012. Mol Psychiatry 2012;17(12):1228–1238.
5. Lerch JP, Worsley K, Shaw WP, et al. Mapping anatomical correlations across cerebral cortex (MACACC) using cortical thickness from MRI. Neuroimage 2006;31(3):993–1003.
6. Evans AC. Networks of anatomical covariance. Neuroimage 2013;80:489–504.
7. Zugman A, Assunção I, Vieira G, et al. Structural covariance in schizophrenia and first-episode psychosis: An approach based on graph analysis. J Psychiatr Res 2015;71:89–96.
8. Palaniyappan L, Park B, Balain V, Dangi R, Liddle P. Abnormalities in structural covariance of cortical gyrification in schizophrenia. Brain Struct Funct 2015;220(4):2059–2071.
9. Chen X, Jiang Y, Chen L, et al. Altered Hippocampo-Cerebello-Cortical Circuit in Schizophrenia by a Spatiotemporal Consistency and Causal Connectivity Analysis. Front Neurosci 2017;11:25.
10. Jiang Y, Duan M, Chen X, et al. Common and distinct dysfunctional patterns contribute to triple network model in schizophrenia and depression: A preliminary study. Prog Neuropsychopharmacol Biol Psychiatry 2017;79(Pt B):302–310.
11. Liao W, Qiu C, Gentili C, et al. Altered effective connectivity network of the amygdala in social anxiety disorder: a resting-state FMRI study. PLoS One 2010;5(12):e15238.
12. Luo C, Yang F, Deng J, et al. Altered functional and effective connectivity in anticorrelated intrinsic networks in children with benign childhood epilepsy with centrotemporal spikes. Medicine (Baltimore) 2016;95(24):e3831.
13. Zhang Z, Liao W, Xu Q, et al. Hippocampus-associated causal network of structural covariance measuring structural damage progression in temporal lobe epilepsy. Hum Brain Mapp 2017;38(2):753–766.
14. Andreasen NC, Pressler M, Nopoulos P, Miller D, Ho BC. Antipsychotic dose equivalents and dose-years: a standardized method for comparing exposure to different drugs. Biol Psychiatry 2010;67(3):255–262.
15. Duan M, Chen X, He H, et al. Altered Basal Ganglia Network Integration in Schizophrenia. Front Hum Neurosci 2015;9:561.
16. Chen X, Duan M, Xie Q, et al. Functional disconnection between the visual cortex and the sensorimotor cortex suggests a potential mechanism for self-disorder in schizophrenia. Schizophr Res 2015;166(1-3):151–157.
17. Chen X, Duan M, He H, et al. Functional abnormalities of the right posterior insula are related to the altered self-experience in schizophrenia. Psychiatry Res 2016;256:26–32.

18. Ridgway GR, Omar R, Ourselin S, Hill DL, Warren JD, Fox NC. Issues with threshold masking in voxel-based morphometry of atrophied brains. Neuroimage 2009;44(1):99–111.

19. Palaniyappan L, Simmonite M, White TP, Liddle EB, Liddle PF. Neural primacy of the salience processing system in schizophrenia. Neuron 2013;79(4):814–828.

20. Olabi B, Ellison-Wright I, McIntosh AM, Wood SJ, Bullmore E, Lawrie SM. Are there progressive brain changes in schizophrenia? A meta-analysis of structural magnetic resonance imaging studies. Biol Psychiatry 2011;70(1):88–96.

21. Gong Q, Lui S, Sweeney JA. A Selective Review of Cerebral Abnormalities in Patients With First-Episode Schizophrenia Before and After Treatment. Am J Psychiatry 2016;173(3):232–243.

22. Dietsche B, Kircher T, Falkenberg I. Structural brain changes in schizophrenia at different stages of the illness: A selective review of longitudinal magnetic resonance imaging studies. Aust N Z J Psychiatry 2017;51(5):500–508.

23. Andreasen NC, Nopoulos P, Magnotta V, Pierson R, Ziebell S, Ho BC. Progressive brain change in schizophrenia: a prospective longitudinal study of first-episode schizophrenia. Biol Psychiatry 2011;70(7):672–679.

24. Gutiérrez-Galve L, Chu EM, Leeson VC, et al. A longitudinal study of cortical changes and their cognitive correlates in patients followed up after first-episode psychosis. Psychol Med 2015;45(1):205–216.

25. Keller A, Castellanos FX, Vaituzis AC, Jeffries NO, Giedd JN, Rapoport JL. Progressive loss of cerebellar volume in childhood-onset schizophrenia. Am J Psychiatry 2003;160(1):128–133.

26. Kubota M, van Haren NE, Haijma SV, et al. Association of IQ Changes and Progressive Brain Changes in Patients With Schizophrenia. JAMA Psychiatry 2015;72(8):803–812.

27. Tanskanen P, Ridler K, Murray GK, et al. Morphometric brain abnormalities in schizophrenia in a population-based sample: relationship to duration of illness. Schizophr Bull 2010;36(4):766–777.

28. van Haren NE, Hulshoff Pol HE, Schnack HG, et al. Progressive brain volume loss in schizophrenia over the course of the illness: evidence of maturational abnormalities in early adulthood. Biol Psychiatry 2008;63(1):106–113.

29. Anderson VM, Goldstein ME, Kydd RR, Russell BR. Extensive gray matter volume reduction in treatment-resistant schizophrenia. Int J Neuropsychopharmacol 2015;18(7):pyv016.

30. van Haren NE, Cahn W, Hulshoff Pol HE, Kahn RS. The course of brain abnormalities in schizophrenia: can we slow the progression? J Psychopharmacol 2012;26(5 Suppl):8–14.

31. Vita A, De Peri L, Deste G, Sacchetti E. Progressive loss of cortical gray matter in schizophrenia: a meta-analysis and meta-regression of longitudinal MRI studies. Transl Psychiatry 2012;2(11):e190.

32. Pergola G, Selvaggi P, Trizio S, Bertolino A, Blasi G. The role of the thalamus in schizophrenia from a neuroimaging perspective. Neurosci Biobehav Rev 2015;54:57–75.

33. Byne W, Hazlett EA, Buchsbaum MS, Kemether E. The thalamus and schizophrenia: current status of research. Acta Neuropathol (Berl) 2009;117(4):347–368.

34. Guillery RW, Harting JK. Structure and connections of the thalamic reticular nucleus: Advancing views over half a century. J Comp Neurol 2003;463(4):360–371.

35. Shepherd AM, Laurens KR, Matheson SL, Carr VJ, Green MJ. Systematic meta-review and quality assessment of the structural brain alterations in schizophrenia. Neurosci Biobehav Rev 2012;36(4):1342–1356.

36. Marenco S, Stein JL, Savostyanova AA, et al. Investigation of anatomical thalamocortical connectivity and FMRI activation in schizophrenia. Neuropsychopharmacology 2012;37(2):499–507.